Rare Metal Materials and Engineering
Volume 51, Issue 6, June 2022
Available online at www.rmme.ac.cn

Science Press

Cite this article as: Wang Zhenguo, Cheng Xi, Liu Wei, et al. Corrosion, Wear and Tribocorrosion Behavior of a New Biomedical Ti-20Zr-10Nb Alloy[J]. Rare Metal Materials and Engineering, 2022, 51(06): 1972-1978.

ARTICLE

Corrosion, Wear and Tribocorrosion Behavior of a New Biomedical Ti-20Zr-10Nb Alloy

Wang Zhenguo[1], Cheng Xi[1], Liu Wei[1], Pan Chao[1], Li Yan[2], Zheng Ziqin[3]

[1] Beijing Chunlizhengda Medical Instruments Co., Ltd, Beijing 101100, China; [2] School of Materials Science and Engineering, Beihang University, Beijing 100191, China; [3] Yantai Branch of China North Industries Group Corporation No. 52 Institute Co., Ltd, Yantai 264003, China

Abstract: The corrosion, wear and tribocorrosion behavior of a new biomedical Ti-20Zr-10Nb alloy was investigated using electrochemical measurements, tribological tests and scanning electron microscopy (SEM). Potentiodynamic polarization tests show that the corrosion potential (E_{corr}) shifts towards negative values and that the corrosion current density (i_{corr}) is increased by two orders of magnitude; these trends differ from those observed with static corrosion. The wear and tribocorrosion results indicate that the wear volume of the Ti-20Zr-10Nb alloy increases with increasing applied load. The contribution of mechanical wear to the material loss of tribocorrosion is greater than that of corrosion. However, the friction coefficients obtained under conditions of electrochemical corrosion are lower than that obtained only under wear. Through observation of the wear crack, it is determined that abrasive wear mechanism is the main mechanism of tribocorrosion. The effect of abrasive particles on the wear and tribocorrosion behavior is considered, and it is found that material loss increases due to particle damage.

Key words: biomedical material; Ti-20Zr-10Nb; tribocorrosion; wear; corrosion

Among metallic biomedical materials, Ti and its alloys have emerged as the first choice for orthopedic implant materials due to their excellent comprehensive properties of high specific strength, low elastic modulus, excellent corrosion resistance, complete inertness to the body's environment and superior biocompatibility to other metallic implant materials, such as stainless steels and Co-Cr alloys[1-4]. Although CP-Ti and Ti-6Al-4V (ELI) have been widely used as biomedical materials, deeper investigations are still required to increase their reliability in the human body during long-term service[4]. To date, new biomedical β titanium alloys with nontoxic alloying elements, appropriate mechanical properties, and excellent biocompatibility have been rapidly developed. Hence, safe and biocompatible elements are preferred when designing new biomedical β titanium alloys, such as Zr, Nb, Ta and Sn elements[3,5].

Ti-Zr-Nb system alloys were developed as promising biocompatible metallic materials for biomedical usage, including Ti-30Zr-xNb (x=5, 7, 9, 10, 13, at%)[6-8], Ti-20Zr-10Nb[9,10], Ti-18Zr-4Nb[11-13], and Ti-15Zr-10Nb[14]. Optimal alloying with Zr and Nb elements provides the possibility of obtaining a metastable β-solid solution after quenching; such a solution has a sufficiently low elastic modulus less than 39 GPa[11], very close to that of human bone (10~30 GPa)[1]. This is very important for metallic biomedical materials because biomechanical compatibility is necessary for implants. In addition, the phase transformation[6-8,15,16], microstructure evolution[7,8,10-14], mechanical properties[11-14], surface and electrochemical characterization[14], and tribological behavior[9] of Ti-Zr-Nb system alloys were also investigated.

However, the service life of metallic implants is determined by their wear and corrosion or tribocorrosion resistance[1-4,17]. Metallic implants undergo corrosion in the human body, leading to wear debris and/or the release of toxic or incompatible metal ions, which may cause allergic and toxic reactions[4,17]. Hence, the designed biomedical β titanium alloys are also expected to have both good corrosion and wear resistance, aiming to maximize the service life of titanium alloy implants in the body. Villanueva et al[17] summarized the relevant literature and showed that corrosion, tribology, and

Received date: June 21, 2021
Foundation item: National Key R&D Program of China (2018YFC1106600)
Corresponding author: Wang Zhenguo, Ph. D., Senior Engineer, Beijing Chunlizhengda Medical Instruments Co., Ltd, Beijing 101100, P. R. China, E-mail: wzghappy@yeah.net

Copyright © 2022, Northwest Institute for Nonferrous Metal Research. Published by Science Press. All rights reserved.

tribocorrosion processes of metallic implant materials are the main concern and driving mechanisms in the degradation processes. The wear, corrosion and tribocorrosion behavior of pure Ti[18], Ti-6Al-4V[19], Ti-30Zr[20,21], Ti-Nb[22,23], Ti-Mo[22,24], Ti-13Nb-13Zr[25], Ti-12Mo-6Zr-2Fe[25], Ti-29Nb-13Ta-4.6Zr[25] and Ti-25Nb-3Mo-3Zr-2Sn alloys[26, 27] have been investigated by different researchers. Yazdi et al[19] investigated the interplay between wear and corrosion during tribocorrosion of an oxygen diffusion layer on Ti-6Al-4V in PBS solution, and the results showed that corrosion has a lower contribution to tribocorrosion rates. Liu et al[20] studied the corrosion and wear behavior of Ti-30Zr alloys, and the results indicated that the wear accelerates corrosion, the corrosion increases the wear, and mechanical wear plays a key role. Wang et al[26, 27] studied the wear, corrosion and tribocorrosion behavior of Ti-25Nb-3Mo-3Zr-2Sn alloy, and the results also indicated that the wear rate of the alloy is mutually affected by both wear and corrosion.

A new biomedical β titanium alloy is considered a new-generation alloy, and the corrosion and wear properties need to be understood. Therefore, the aim of this study is to evaluate the electrochemical corrosion, wear and tribocorrosion behavior of the Ti-20Zr-10Nb alloy in simulated body fluids. The effect of abrasive particles and the interaction of wear and corrosion was considered. According to the experimental results, the wear volume and friction coefficients were acquired, and the wastage and wear-corrosion mechanism were analyzed. Finally the potential medical applications of the Ti-20Zr-10Nb alloy were evaluated.

1 Experiment

1.1 Sample preparation

Ti-20Zr-10Nb (at%) was prepared using high purity (>99.9 wt%) raw materials, including titanium sponges, zirconium sponges and high purity niobium. The ingots (100 g) were re-melted three times for homogeneity through nonconsumable arc-melting method under Ar atmosphere protection, a WS-4 vacuum arc furnace was used, and water-cooled copper was used as the melting crucible. The ingots were solution-treated at 900 °C in a box furnace for 6 h under the vacuum at 5×10^{-3} Pa followed by cooling in a furnace. The density of the alloy was 5.71 g/cm^3. The specimens (30 mm×20 mm×2 mm and 10 mm×10 mm×1 mm) for the wear, corrosion and wear-corrosion tests were wire-electrode cut and gradually ground with SiC proof papers (#200, #400, #600, #800, #1000 and # 1500). Fig. 1 shows the XRD patterns of Ti-20Zr-10Nb alloy with martensite phases with hexagonal (a') and orthorhombic (a") structures.

1.2 Simulated body fluid

Hank's simulated body fluid is commonly used to study the electrochemical corrosion of metal implants. The composition of Hank's simulated body fluid was the same as that in Ref. [28]. Before the tests, the pH of the Hank ' s solution was adjusted to 7.7±0.1 with an acid-base. Normal body temperature ranges from 36.5 °C to 37.5 °C, so the test temperature

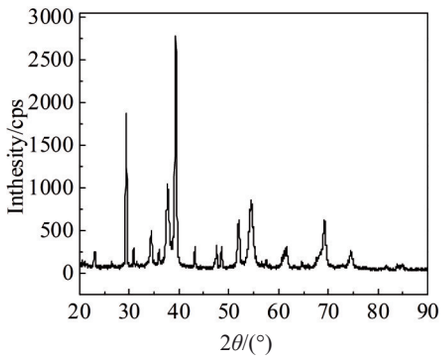

Fig.1 XRD pattern of Ti-20Zr-10Nb alloy after heat treatment under 900 °C/6.0 h/FC

was maintained at 37.0±0.5 °C, and a fresh solution was used for each test.

1.3 Corrosion, wear and tribocorrosion tests

The electrochemical corrosion tests were carried out on a CHI 660C potentiostat (CH, USA) connected to a standard three-electrode system. In the three-electrode system, a saturated calomel electrode (SCE) was used as the reference electrode (RE), a platinum sheet electrode was used as the counter electrode (CE), and the working electrode (WE) was the Ti-20Zr-10Nb sample. During the test, the initial potential was −0.8 V, the final potential was 0.2 V, and the sweep rate was 4.17 mV/s.

The tests were carried out by a TE66 microabrasion tester (Phoenix Tribology, UK). ZrO_2 ceramic balls (Φ25.4 mm) were selected as the friction pair, and the test parameters are listed in Table 1. Abrasive Al_2O_3 particles with a size of 3.0± 0.5 μm were selected. Hank ' s solution with and without abrasives was used during the tests. The Hank ' s solution contained 0.01 g/cm^3 Al_2O_3 particles.

To simulate a physiological human body environment, tribocorrosion tests were conducted in Hank ' s solution. Tribocorrosion experiment tests were carried out on a TE66 microabrasion tester connected to a CHI 660C potentiostat. The test parameters were similar to those listed in Table 1. During the tribocorrosion tests, the initial potential was −2.5 V, the final potential was 1.0 V, and the sweep rate was 14.58 mV/s.

After the wear and tribocorrosion tests, the diameter b of wear scar was measured by a calibrated digital optical microscope (OM, 15JE), and the values were used to calculate the material volume. The corrosion and worn surface were observed through scanning electron microscopy (SEM, JSM-

Table 1 Test parameters of the wear tests

Parameter	Value
Speed of ball rotation/r·min^{-1}	150
Rotating distance/r	600 (equivalent to 47.9 m)
Applied load/N	1.0, 2.0, 3.0, 4.0, 5.0
Particle concentration/g·cm^{-3}	0.01

6010) after the corrosion tests. The wear volume was calculated using the following equation [26]:

$$V=\pi b^4/64R \quad (1)$$

where V, b and R are the wear volume of the wear scar, diameter of the wear scar and diameter of the ZrO_2 ceramic balls (25.4 mm), respectively.

2 Results and Discussion

2.1 Electrochemical corrosion

The electrochemical polarization curve of the Ti-20Zr-10Nb alloy in Hank's solution is shown in Fig. 2, and the values of −0.457 V for corrosion potential (E_{corr}) and 1.089×10^{-7} A/cm^2 for corrosion current density (i_{corr}) are acquired (Table 2). The values of E_{corr} and i_{corr} for different biomedical titanium alloys in Hank's solution, Ti-30Zr[20], Ti-13Nb-13Zr[29], Ti-6Al-4V[30] and Ti-24Nb-4Zr-8Sn[30], are also listed in Table 2. As seen in Table 2, the value of E_{corr} for the Ti-20Zr-10Nb alloy is comparable to that of other biomedical titanium alloys, and the corrosion rate is slightly faster than that of other alloys. The results indicate that the Ti-20Zr-10Nb alloy has a low corrosion tendency. Although the corrosion rate is nearly twice that of other alloys, it is still in the same order of magnitude. SEM images of the Ti-20Zr-10Nb alloy after corrosion tests are shown in Fig. 3, indicating that the corrosion feature is uniform. Uniform corrosion is an important property for metal implant materials.

The favorable corrosion resistance of titanium alloys is attributed to the passive film naturally formed on the surface, while the passive film corrosion resistance greatly relies on the created layer thickness and the natural elements that are present in titanium alloys[31]. The results show that the Ti-20Zr-10Nb alloy is a potential material for biomedical implants from the viewpoint of corrosion.

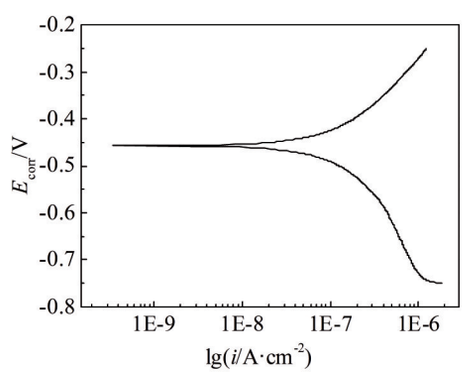

Fig.2 Electrochemical polarization curve of the Ti-20Zr-10Nb alloy in Hank's solution

Table 2 Corrosion potential (E_{corr}) and corrosion current density (i_{corr}) of different titanium alloys

Alloy	E_{corr}/V	i_{corr}/ $\times10^{-8}$ A·cm^{-2}	Simulated body fluids	Ref.
Ti-20Zr-10Nb	−0.457	10.89	Hank's	-
Ti-30Zr	−0.47	5.50	Hank's	[18]
Ti-13Nb-13Zr	−0.47	7.1	Hank's	[27]
Ti-6Al-4V	−0.48	4.2	Hank's	[28]
Ti-24Nb-4Zr-8Sn	−0.60	4.9	Hank's	[28]

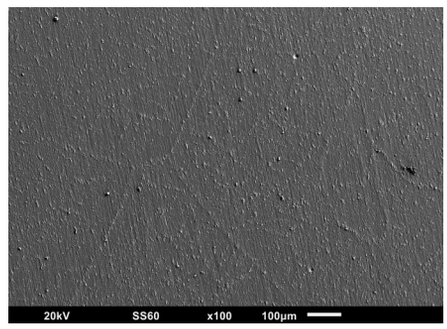

Fig.3 Surface SEM image of Ti-20Zr-10Nb alloy after corrosion

2.2 Wear behavior

Fig. 4 shows the wear volume of the Ti-20Zr-10Nb alloy without electrochemical corrosion. The wear volume is increased with increasing applied load. The results are in accordance with the fundamental laws of wear[32].

The wear volume when particles are present is greater than that without particles under the same experimental conditions. The results indicate that the particles play a role in material loss. When the particle is added between the two friction pairs, the wear mechanism can be changed. Once the abrasive particles or wear debris are bound by two friction pairs, two-body is dominant [33]. As shown in Fig.5, many grooves can be observed on the wear morphology of the Ti-20Zr-10Nb alloy without electrochemical corrosion. The wear morphology is obviously caused by two-body wear. The grooves on the wear surface caused by Al_2O_3 abrasive particle are obviously wide and deep, as shown in Fig. 5b. That is, the two-body wear mechanism is more obvious due to the presence of Al_2O_3 abrasive particles. It has been reported that two-body wear can lead to more damage in the form of material loss [32, 33]. Hence, the wear volume of the sample with particles is higher than without particles. In addition, wear debris is also observed on wear surface. It is clear that the amount of wear debris in the sample with particles (Fig. 5b) is greater than that in the same sample without particles (Fig. 5a).

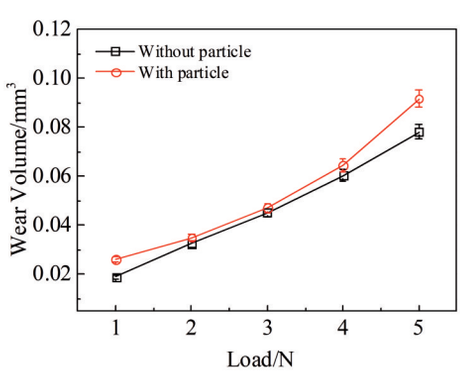

Fig.4 Wear volume of the Ti-20Zr-10Nb alloy without electrochemical corrosion

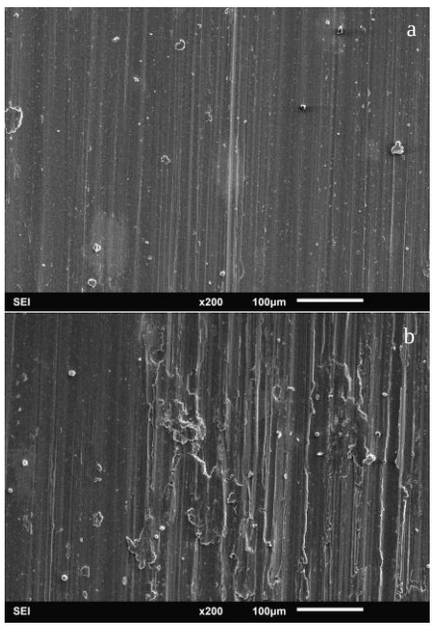

Fig.5 Wear morphologies of the Ti-20Zr-10Nb alloy without electrochemical corrosion: (a) without particles and (b) with particles

Fig.6 shows the average friction coefficient of the Ti-20Zr-10Nb alloy without electrochemical corrosion with/without particles. The average friction coefficients decrease with increasing the applied load. The average friction coefficients obtained with particles are larger than those without particles. The result is consistent with the result of the wear volume experiment, as shown in Fig. 4. Under a larger applied load, there are only small friction coefficients between the two friction pairs due to the small contact area. The addition of abrasive particles can also affect the contact area between the two friction pairs, resulting in an increase in the fluctuation for the friction coefficients. The presence of abrasive particles also affects the formation of passivation film on the wear surface and leads to a higher friction coefficient.

2.3 Tribocorrosion behavior

2.3.1 Electrochemical corrosion with wear

The dynamic electrochemical polarization curves with wear of the Ti-20Zr-10Nb alloy are presented in Fig. 7, and the corresponding corrosion potentials (E_{corr}) and corrosion current densities (i_{corr}) are listed in Table 3. All the curves present similar electrochemical corrosion characteristics. Without the effect of the abrasive Al_2O_3 particles, the maximum E_{corr} value of −0.49 V is obtained at a load of 1.0 N, while the value of −0.89 V is acquired at 5.0 N. This result is similar to that of Ti-30Zr alloy under the same test conditions[21]. The E_{corr} decreases with increasing applied load, and the i_{corr} is on the same order of magnitude. This phenomenon suggests that the corrosion tendency of the Ti-20Zr-10Nb alloy increases with increasing applied load; that is, wear accelerates the corrosion of Ti-20Zr-10Nb alloy under wear-corrosion conditions. In addition, the effect of the applied load on the corrosion potential without added particles is greater than that with added particles. In fact, the presence of the abrasive Al_2O_3 particles affects the contact area between the two friction pairs.

Unlike the trends observed with the static electrochemical corrosion (Fig.2), E_{corr} shifts towards negative values and i_{corr} is

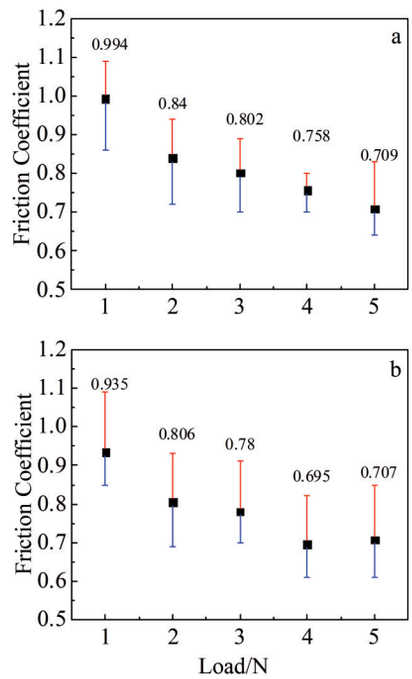

Fig.6 Friction coefficients of the Ti-20Zr-10Nb alloy without electrochemical corrosion: (a) without particles and (b) with particles

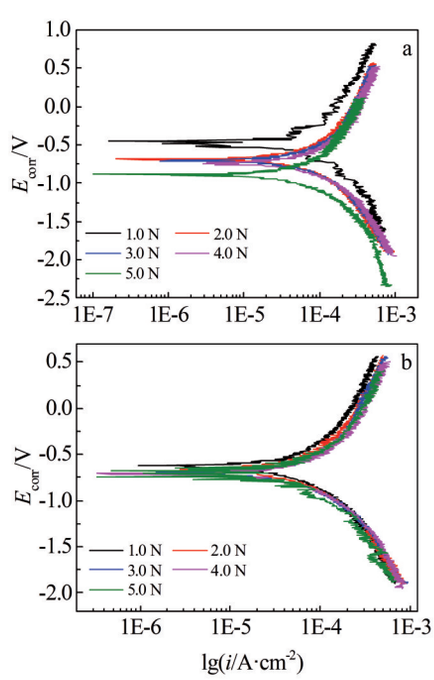

Fig.7 Electrochemical polarization curves with wear of the Ti-20Zr-10Nb alloy: (a) without particles and (b) with particles

Table 3 Corrosion potential (E_{corr}) and corrosion current density (i_{corr}) of Ti-20Zr-10Nb alloy

Load/N	Without particle		With particle	
	E_{corr}/V	i_{corr}/A·cm^{-2}	E_{corr}/V	i_{corr}/A·cm^{-2}
1.0	-0.49	3.20E-5	-0.64	3.17E-5
2.0	-0.69	3.07E-5	-0.66	3.28E-5
3.0	-0.71	2.85E-5	-0.71	3.46E-5
4.0	-0.74	3.13E-5	-0.71	3.66E-5
5.0	-0.89	2.28E-5	-0.71	2.96E-5

increased by two orders of magnitude. The results indicat that the corrosion resistance of the Ti-20Zr-10Nb alloy decreases due to wear processing. That is, wear accelerates the corrosion. In addition, the polarization curves demonstrate greater fluctuations; this phenomenon reflects the tribocorrosion process. The fluctuations of the polarization curves are also related to the process of passivation film formation and destruction, due to the dynamic balance between the rapid repassivation form and mechanical removal in the wear surface[33,34]. Under the tribocorrosion test conditions, the passivation film is easily formed due to electrochemical corrosion and easily damaged and delaminated from the wear surface due to the wear[26,32].

2.3.2 Wear behavior with electrochemical corrosion

When the tests were processed under electrochemical corrosion conditions, the wear volume of the Ti-20Zr-10Nb alloy is retained regardless of the presence of added particles, as shown in Fig.8. The wear volume increases with increasing applied load, similar to the trend in Fig.4. Compared with the data shown in Fig. 4, the wear volume of the alloy with electrochemical corrosion is higher under the same test conditions. When the test is processed without abrasive Al_2O_3 particles, the wear volume of the Ti-20Zr-10Nb alloy with corrosion is 1.16~1.46 times larger than that of the alloy without corrosion. With the abrasive Al_2O_3 particles, the wear volume of the Ti-20Zr-10Nb alloy with corrosion is 1.17~1.57 times larger than that of the alloy without corrosion. Interestingly, regardless of the presence or absence of abrasive Al_2O_3 particles, the maximum multiple occurs at 3 N and the minimum multiple occurs at 1 N. The results indicate that electrochemical corrosion is contributed to material loss. In addition, the applied load of 3 N may be a turning point in the wear mechanism.

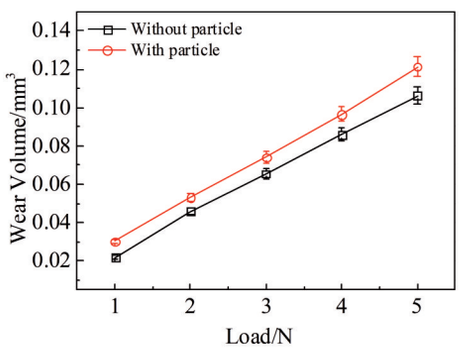

Fig.8 Wear volume of the Ti-20Zr-10Nb alloy with electrochemical corrosion

Under electrochemical corrosion conditions, the average friction coefficients of the Ti-20Zr-10Nb alloy with and without particles are shown in Fig.9. The value of the average friction coefficient (ranging from 0.45 to 0.54) is lower than that without corrosion, and the values have a smaller range of fluctuations. This phenomenon indicates that electrochemical corrosion changes the lubrication state between the two friction pairs. The change in lubrication state is related to the passivation film or corrosion products on the worn surface, and the passivation film or corrosion products can act as a lubricant and have a protective effect [19, 25].

The wear morphologies of the Ti-20Zr-10Nb alloy after electrochemical corrosion without/with Al_2O_3 abrasive particles are shown in Fig.10. There are some parallel grooves along the sliding direction on the Ti-20Zr-10Nb worn alloy surface, which is a typical characteristic feature of abrasive wear. The occurrence of an abrasive wear mechanism is related to the low hardness and high plasticity of the Ti-20Zr-10Nb alloy [19]. Through observation of the worn surface, it is determined that the abrasive wear mechanism is the main mechanism of tribocorrosion.

Besides, the wear debris is also observed on the worn surface in Fig. 10. These wear debris at anodic potential are corrosion products[25]. It is reported that titanium alloys experience lower wear rate and material loss due to the lubricating behavior of corrosion products (third body effect) [25]. Some

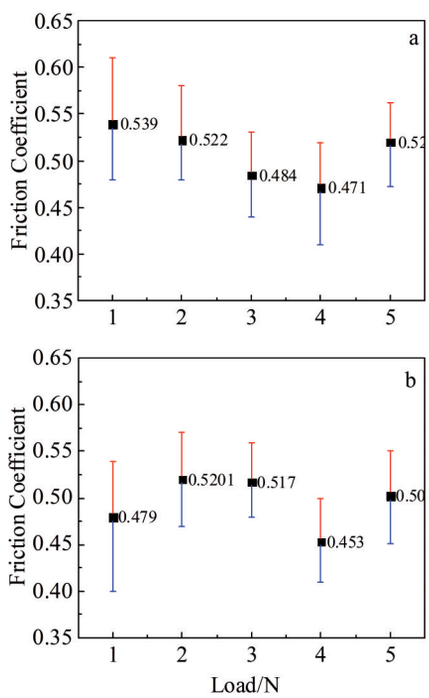

Fig.9 Friction coefficients of the Ti-20Zr-10Nb alloy with electrochemical corrosion: (a) without particles and (b) with particles

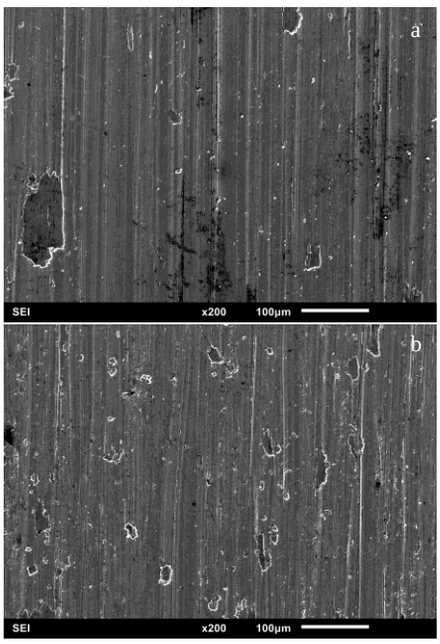

Fig.10 Wear morphologies of the Ti-20Zr-10Nb alloy after electrochemical corrosion: (a) without particles and (b) with particles

EDS results reveal that worn surface layer has high oxygen content for the titanium alloys[19,24,25,35]. The presence of O indicates that the tribolayers are oxidized due to the electrochemical reaction during the process of wear in the simulated body fluid[35]. There are similar results or phenomena for biomedical titanium alloys, that is, the biomedical titanium alloys are more susceptible to the chemical attack from the corrosive fluid (Hank's solution in this study).

2.3.3 Variation of W_{ac}, W_a and W_c

It is well known that the synergistic interactions between electrochemical corrosion and mechanical wear usually result in an increased material loss compared to individual electrochemical corrosion or mechanical wear[21,26,32]. Hence, the synergistic interactions between corrosion and wear need to be understood because implant materials are easily subjected to relative movements in a corrosive body environment.

Therefore, the total material loss induced by the synergistic effect of wear and corrosion can be expressed through Eq.(2)[26,32]:

$$W_{ac}=W_c+W_a \quad (2)$$

where W_{ac} is the total material loss (g) and W_a is the material loss induced by wear; W_c can be calculated through Faraday's law:

$$W_c=Q/ZF=Mit/ZF \quad (3)$$

where Q is the charge passed, Z is the number of electrons involved in the corrosion process, F is Faraday's constant (96 500 C/mol), i is the corrosion current, t is the test time of tribocorrosion and M is the atomic mass of the alloy.

The values of the W_{ac}, W_a and W_c are obtained from Eq.(2) and Eq.(3), as listed in Table 4.

Table 4 Variation of W_{ac}, W_a and W_c of the Ti-20Zr-10Nb alloy

Load/N	Without particle			With particle		
	W_{ac}/ $\times10^{-4}$ g	W_c/ $\times10^{-6}$ g	W_a/ $\times10^{-4}$ g	W_{ac}/ $\times10^{-4}$ g	W_c/ $\times10^{-6}$ g	W_a/ $\times10^{-4}$ g
1.0	1.25	1.18	1.24	1.73	1.17	1.72
2.0	2.62	1.14	2.61	3.04	1.21	3.03
3.0	3.74	1.06	3.73	4.23	1.28	4.22
4.0	4.90	1.16	4.89	5.51	1.36	5.50
5.0	1.25	1.18	1.24	1.73	1.17	1.72

Based on the values of W_{ac}, the wastage map of the Ti-20Zr-10Nb alloy is constructed. The wastage map can be divided into three areas: low, medium and high (Eq.(4~6)). It is clear that there are only high wastage areas for the Ti-20Zr-10Nb alloy under the test conditions in this study. It is not necessary to draw the wastage map.

$W_{ac}\leqslant3.0\times10^{-5}$ g Low (4)

3.0×10^{-5} g$<W_{ac}\leqslant6.0\times10^{-5}$ g Medium (5)

$W_{ac}>6.0\times10^{-5}$ g High (6)

The results in Table 4 also show that the value of W_a is 2 orders of magnitude higher than that of W_c. It has been proposed that a W_a/W_c value more than 10 is a quantitative criterion to indicate that tribocorrosion is dominantly controlled by a mechanical wear mechanism rather than corrosion and wear/corrosion mechanisms[26,32]. Therefore, mechanical wear plays a role in material loss during the tribocorrosion test.

3 Conclusions

1) Under the corrosive conditions of a human body, the applied load, abrasive particles or wear debris can affect the tribocorrosion behavior of the Ti-20Zr-10Nb alloy.

2) Because of the interaction between the wear and corrosion, the corrosion potential (E_{corr}) shifts towards negative values, and the corrosion current density (i_{corr}) is increased by two orders of magnitude compared with that of static corrosion.

3) Mechanical wear plays the role of material loss. Hence, the abrasive wear mechanism is the main mechanism of tribocorrosion.

References

1 Zhang C L, Bao X Y, Zhang J Y *et al. Rare Metal Materials and Engineering* [J], 2021, 50(2): 717

2 Bahl S, Suwas S, Chatterjee K. *International Materials Reviews* [J], 2021, 66(2): 114

3 Kaur M, Singh K. *Materials Science and Engineering C*[J], 2019, 102: 844

4 Zhang L, Chen L. *Advanced Engineering Materials*[J], 2019, 21: 1 801 215

5 Zhu K P, Zhu J W, Qu H L. *Rare Metal Materials and Engineering*[J], 2012, 41(11): 2058

6 Song X, Xiong C, Zhang F *et al. Materials Letters*[J], 2020, 259: 126 914
7 Qu W, Sun X, Yuan B *et al. Materials Characterization*[J], 2017, 126: 81
8 Qu W, Sun X, Yuan B *et al. Materials Characterization*[J], 2016, 122: 1
9 Qu W, Sun X, Yuan B *et al. Rare Metals*[J], 2017, 36: 478
10 Cui Y, Li Y, Luo K *et al*. *Materials Science and Engineering A* [J], 2010, 527(3): 652
11 Sheremet'ev V A, Kudryashova A A, Dinh S T *et al. Metallurgist* [J], 2019, 63: 51
12 Kreitcberg A, Brailovski V, Prokoshkin S. *Journal of Materials Processing Technology*[J], 2018, 252: 821
13 Konopatsky A S, Dubinskiy S M, Zhukova Y S *et al. Materials Science and Engineering A*[J], 2017, 702: 301
14 Calderon-Moreno J M, Vasilescu C, Drob S I *et al. Journal of Alloys and Compounds*[J], 2014, 612: 398
15 Qu W T, Gong H, Wang J *et al. Rare Metals*[J], 2019, 38: 965
16 Xue P F, Li Y, Zhang F *et al. Scripta Materialia*[J], 2015, 101: 99
17 Villanueva J, Trino L, Thomas J *et al. Journal of Bio- and Tribo-Corrosion* [J], 2017, 3: 1
18 Liamas E, Thomas O, Muoz A I *et al. Journal of the Mechanical Behavior of Biomedical Materials*[J], 2020, 102: 103 511
19 Yazdi R, Ghasemi H M, Abedini M *et al. Applied Surface Science*[J], 2020, 5181: 46 048
20 Liu M, Wang Z, Shi C *et al. Materials Research Express*[J], 2019, 6: 8658
21 Wang Z, Zhou Y, Wang H *et al. Materials Letters*[J], 2018, 218: 190
22 Ureña J, Tsipas S, Pinto A M *et al. Corrosion Science*[J], 2018, 140: 51
23 Çaha I, Alves A C, Kuroda P A B *et al. Corrosion Science*[J], 2020, 167: 108 488
24 Xu W, Chen M, Lu X *et al. Corrosion Science*[J], 2020, 168: 108 557
25 Neto M Q, Rainforth W M. *Biotribology* [J], 2020, 24: 100 141
26 Wang Z, Huang W, Li Y *et al. Materials Science and Engineering C*[J], 2017, 76: 1094
27 Huang W, Wang Z, Liu C *et al. Journal of Bio- and Tribo-Corrosion*[J], 2015, 1: 1
28 Wang Z, Huang W, Meng X. *Materials Science and Technology* [J], 2015, 31: 1335
29 Suresh K S, Geetha M, Richard C *et al. Materials Science and Engineering C*[J], 2012, 32: 763
30 Bai Y, Hao Y L, Li S J *et al. Materials Science and Engineering C*[J], 2013, 33: 2159
31 Manam N S, Harun W S W, Shri D N A *et al. Journal of Alloys and Compounds*[J], 2018, 701: 698
32 Wang Z, Li Y, Huang W *et al. Journal of the Mechanical Behavior of Biomedical Materials* [J], 2016, 63: 361
33 Wang Z, Huang W, Ma Y. *Materials Science and Engineering C* [J], 2014, 42: 211
34 Li K M, Song K J, Guan J *et al. Surface and Coatings Technology* [J], 2020, 386: 125 506
35 Hua N B, Hong X S, Lin L Y *et al. Journal of Non-Crystalline Solids*[J], 2020, 543: 120 116

一种新型生物医用 Ti-20Zr-10Nb 合金的腐蚀、磨损及腐蚀磨损行为

王振国[1]，程　曦[1]，刘　伟[1]，潘　超[1]，李　岩[2]，郑自芹[3]

(1. 北京市春立正达医疗器械股份有限公司，北京 101100)

(2. 北京航空航天大学 材料科学与工程学院，北京 100191)

(3. 中国兵器工业第五二研究所烟台分所有限责任公司，山东 烟台 264003)

摘　要：通过电化学腐蚀、摩擦学测试以及扫描电镜（SEM）观察等方法，研究了新型生物医用 Ti-20Zr-10Nb 合金的腐蚀、磨损以及腐蚀磨损行为。动电位极化实验结果表明，与静态腐蚀相比，腐蚀电位（E_{corr}）向负值偏移，腐蚀电流密度（i_{corr}）增加了 2 个数量级。磨损和腐蚀磨损结果显示，Ti-20Zr-10Nb 合金的磨损体积随载荷的增加而增大。研究结果表明，机械磨损在腐蚀磨损中对材料的流失贡献大于腐蚀的贡献。电化学腐蚀条件下的摩擦系数均低于纯磨损条件下获得的摩擦系数。通过观察腐蚀磨损后的形貌可知，磨粒磨损为腐蚀磨损中的主要磨损机制。此外还验证了磨粒的添加对磨损和腐蚀磨损行为的影响，发现磨粒的添加会增加材料的流失。

关键词：生物医用材料；Ti-20Zr-10Nb；腐蚀磨损；磨损；腐蚀

作者简介：王振国，男，1983 年生，博士，高级工程师，北京市春立正达医疗器械股份有限公司，北京 101100，E-mail：wzghappy@yeah.net